Characterization of Rapid Alkalinization Factors (RALFs) in *Physcomitrium patens*

(ヒメツリガネゴケにおける **RALF** ペプチドホルモンの解析**)**

By
Eggie Febrianto Ginanjar

A Dissertation

Submitted to Graduate School of Life Science Hokkaido University in partial fulfillment of the requirement for the degree of Doctoral Philosophy in Life Science

Graduate School of Life Science
Hokkaido University, Sapporo, Japan

March 2022

Characterization of Rapid Alkalinization Factors (RALFs) in *Physcomitrium patens*

By
Eggie Febrianto Ginanjar

Graduate School of Life Science
Hokkaido University, Sapporo, Japan

March 2022

Acknowledgments

I would first like to thank to Prof. Tomomichi Fujita for accepting me to peruse Doctoral Degree in his Laboratory, and teaching me about research in molecular plant physiology and plant development. Prof. Fujita office is always open whenever I have a question about my research.

I would also like to thank to Dr. Ooi-Kock Teh who gave me a lot of advices, guidance, encouragement and teaches me in experimental laboratory during my study.

I would also like to acknowledge Prof. Tanaka Kazuma and Dr. Takeo Sato as the co-supervisor for my dissertation, and I am gratefully indebted to theirs very valuable comments on this dissertation and my study.

I would also like to thank to Dr. Satoshi Naramoto and all members of Fujita laboratory and Watahiki Laboratory for their kindness and hospitality. Miss. Chiyo Jinno and Mr. Maki Yokoi also helped me as translator if I did not understand about Japanese.

I must express my very profound gratitude to my family for providing me with unfailing support and continuous encouragement throughout my years of study and through the process of researching and writing this dissertation. This accomplishment would not have been possible without them.

Finally, I would like to thank the Japanese government (Monbukagakusho:MEXT) scholarship program for providing the wonderful opportunity to study in Hokkaido University, Japan.

Table of Contents

Acknowledgments 2
1. Introduction 4
1.1. *Phycomitrium patens* (*P. patens*) as a model to study evolutionary and developmental biology 4
1.2. Life cycle of *P. patens* 4
1.3. RALFs are small peptides that act as growth regulators in plants 5
2. Aim of the study 7
3. Materials and methods 8
3.1. Plant materials and growth conditions 8
3.2. Cell number and length observation 9
3.3. Microscopic observation and statistical analysis 10
3.4. Immunoblotting 10
4. Result 11
4.1. Disruption of PpRALF1 and PpRALF2 in *P.patens* impairs protonemal development 11
4.2. Disruption of PpRALF1 or PpRALF2 reduces cell length and cell number in chloronema cells 13
4.3. Overexpression of PpRALF1 and PpRALF2 impaired chloronemal cell length and highlighted their overlapping roles in chloronema tip growth. 14
4.4. PpRALF1 and PpRALF2 displayed different localization demonstrating their involvement in facilitating protonema tip growth. 17
4.5. Proteolytic cleavage of PpRALF1 is necessary for its function 18
5. Discussion 19
6. Conclusion 22
7. Reference 23
8. Figures 27
9. Supporting figures 43
10. Supporting tables 45
11. Abbreviations 47

1. Introduction

1.1. *Phycomitrium patens* (*P. patens*) as a model to study evolutionary and developmental biology

The moss *P. patens* Gransden was established as a model species since 1962 (Cove et al., 2009; Rensing et al., 2008). This moss can be easily cultured in the laboratory and spends majority of its life cycle in a haploid state, giving advantage for application of experimental techniques similar to those used in microbes and yeast (Cove, 2005; Cove et al., 2009). Furthermore, developmental processes of the *P. patens* are relatively simple, and it generates only a few tissues that contain a limited number of cell types (Cove et al., 2009). Interestingly, Rensing et al (2008) reported that *P. patens* shares fundamental genetic and physiological processes with vascular plants. In another word, because gene families encoding the basic developmental 'tool kit' in flowering plants are conserved in the *P. patens* genome, *P. patens* is rendered as a powerful model plant system in evolutionary and developmental biology (Prigge & Bezanilla, 2010; Rensing et al., 2008).

1.2. Life cycle of *P. patens*

P. patens has a simple life cycle. Like vascular plants, the life cycle of *P. patens* exhibits alteration between haploid gametophyte and diploid sporophyte generation. However, unlike vascular plants, the haploid generation of *P.patens* is a dominant cycle. The first phase in the haploid generation is protonema. Protonema cells are multicellular filamentous, two-dimensional systems or network that develops when haploid spores germinate and is comprised of two filament types called chloronema and caulonema (Jang & Dolan, 2011; Prigge & Bezanilla, 2010).

The first cell type to emerge from the spore is the chloronema. This chloronema undergoes tip growth and continuously produces chloronemal cells to form a filamentous body (Kofuji & Hasebe, 2014; Menand et al., 2007). The features of chloronemal cells are slow-growing and contain a lot of large round chloroplasts and the cell plates that form are oriented perpendicular to the growth axis. As the plant continues to grow, chloronema apical cells will differentiate into caulonema apical cells that produce caulonemal cells. These caulonemal cells are characterized by a more rapid growth, less-green chloroplasts, and cell plates that form an oblique angle to the long axis of the cell (Kofuji & Hasebe, 2014; Menand et al., 2007).

When moss becomes mature, caulonema cells form side branch initial cells, and there is a transition in the side branch formation from chloronemal filaments to gametophore initials which later develop into gametophores. Kofuji and Hasebe (2014) reported that only 5% of the caulonemata cells form gametophores. On top of the gametophores, sex organs antheridia and archegonia will form. Upon sex organ maturation, flagellate sperm will be released from the archegonia to fertilize the egg cell within an archegonium. After fertilization, zygotes develop into diploid embryonic sporophytes that produce spores.

1.3. RALFs are small peptides that act as growth regulators in plants

Plant growth and development are influenced by environmental and endogenous signals. One of the important endogenous signals for cell-to-cell communication is small signaling peptides (Murphy et al., 2012). Studies of many small peptides have been shown that they are involved in almost all developmental processes. Among the many signaling peptides discovered, the rapid alkalinization factor (RALF) family has been linked to several physiological and developmental processes such as cell expansion (Haruta et al., 2014), lateral root development

(Gonneau et al., 2018; Murphy et al., 2016), root hair growth (Wu et al., 2007), pollen tube elongation (Covey et al., 2010) and immunity (Stegmann et al., 2017) (Czyzewicz et al., 2013; Murphy & De Smet, 2014).

The RALF peptide family was discovered over two decades ago (Pearce et al., 2001). It was identified as a 5-kD secreted peptide from tobacco leaves that can be induced by a rapid alkalinization of the tobacco cell cultures. Not only in tobacco, RALFs are present in a large number of plant species from dicots to monocots and gymnosperms, indicating a fundamental role in plant evolution (Campbell & Turner, 2017; Cao & Shi, 2012; Pearce et al., 2001; Sharma et al., 2016). Of the 37 RALF genes encoded in *Arabidopsis thaliana* genome, the primary functions of several RALFs are inhibition of cell elongation (Abarca et al., 2021; Haruta et al., 2014; Pearce et al., 2001) and cell division (Gonneau et al., 2018; Murphy et al., 2016).

Generally RALF-encoding transcripts are translated as pre-pro-proteins and are activated in the apoplast through proteolytic cleavage by a serine protease (S1P) at an RRXL motif (Srivastava et al., 2009). The mature RALF peptide contains approximately 50 amino acids with four highly conserved cysteine residues. These conserved cysteines are important for forming disulfide bridges and for correct conformational folding of the mature peptide. Reduction of the disulfide bridge inactives the RALFs and led to diminished alkalinization activity (Pearce et al., 2001). Moreover, the mature peptide also contains a functionally conserved YISY motif. This motif is vital for an effective binding between RALF and its receptor (Pearce et al., 2010).

Signaling peptides specifically bind to the extracellular domain of receptors, and so far in *Arabidposis* receptors for the peptide signaling that have been identified are members of the receptor-like kinase (RLK) family (Oh et al., 2018). Haruta et al (2014) has identified FERONIA (FER), a receptor-kinase from the Catharantus roseus RLK1-like (CrRLK1L) subfamily, as the

first RLK for AtRALF1 and has confirmed that FERONIA is involved in the rapid alkalization response. RALF is able to suppresses cell elongation of the primary root by activating the cell surface-localised FER in *A. thaliana* (Haruta et al., 2014). This finding emphasized the canonical role of RALF1 in arresting root growth development in tomato and Arabidopsis (Pearce et al., 2001).

The RALF gene family is essential for the plant growth and development. However, there is no report in non-seed plants. In *P patens*, the *RALF* family is predicted to consist of three copies (Pp3c3_15280, Pp3c6_7200 and Pp3c25_4180). Unlike the vascular plants in which the *RALF genes* family has greatly expanded (4 in *Vitis vinifera*, 37 in *A. thaliana*) (Murphy & De Smet, 2014), the lower number of *RALFs* genes in *P. patens* allow me to investigate their ancestral and canonical roles.

2. Aim of the study

RALF functions are mostly reported in angiosperms. Although it has been revealed that RALFs peptides are important in angiosperms, it remains unknown about their roles in early diverging land plants which have no root growth development process. This study aims to characterize and investigate what their functional roles are in early land plants.

3. Materials and methods

3.1. Plant materials and growth conditions

The moss *P. patens* Bruch and Schimp. *subsp. patens* collected in Gransden Woods (Ashton & Cove, 1977) was used as the wild-type line. In this study, I also used six KO mutants which were *Ppralf1, Ppralf2, Ppralf3, Ppralf1.ralf2dko, Ppralf2.3dko* and *Ppralf1.2.3tko*. The single knockout mutants *Ppralf1* and *Ppralf2,* and double knockout mutants *Ppralf1.Ppralf2* dko were kindly given by Dr. Ooi Kock Teh. Another knockout mutant had been generated by preparing 1.5kb of the 5' and 3'homologous regions (HR) that were PCR-amplified from genomic DNA with PrimeSTAR Max DNA polymerase (Takara) (Ginanjar et al., under revision). The HR fragments of PpRALF1, PpRALF2 and PpRALF3 were cloned into pTN182, p35S-Zeo or pTN186 vectors, respectively, using the Hot Fusion method (Fu et al., 2014). Strategy of homologous recombination to generate knock-out mutants was described in Ginanjar et al (under revision). All knock out mutants have been generated by homologous recombination and screened via PCR for verification of disruption of the wild-type *PpRALF* locus as well as correct 5' and 3' integration of the construct with primers that bind outside of the introduced construct and inside the selection cassette (Table S1).

All plant materials were cultivated on BCDAT (BCD medium contains 1 mM $MgSO_4$, 10 mM KNO_3, 45 µM $FeSO_4$, 1.8 mM KH_2PO_4 (pH 6.5 adjusted with KOH), and trace element solution (alternative TES ; 0.22 µM $CuSO_4$, 0.19 µM $ZnSO_4$, 10 µM H_3BO_3, 0.10 µM Na_2MoO_4, 2 µM MnCl2, 0.23 µM $CoCl_2$, and 0.17 µM KI)) agar medium and grew under continuous white light at 25ºC as described previously (Nishiyama et al., 2000). To observe phenotype and gametophore number between WT, *ralf* knock-out mutants or iOX lines (strong iOX:PpRALF1-Citrine line (#1), weak iOX:PpRALF1-Citrine line (#2), strong iOX:PpRALF2-Citrine line (#17)

and weak iOX:PpRALF2-Citrine line (#22) (kindly given by Dr. Ooi Kock Teh and also used in Ginanjar et al. under revision)), I regenerated plants from single protoplasts. Protoplasts prepared by driselase treatment were washed three times with 8% mannitol solution (Nishiyama et al., 2000). Protoplast solution was mixed with PRMT (BCD medium supplemented with 5 mM ammonium tartrate, 10 mM $CaCl_2$, 0.8% agar, and 8% mannitol) and plated onto a cellophane-covered PRMB (BCD medium supplemented with 5 mM ammonium tartrate, 10 mM $CaCl_2$, 0.8% agar, and 6% mannitol) (Nishiyama et al., 2000). After incubation for 2-3 d under continuous light, the cellophane was transferred to a fresh BCDAT plate and incubated for 5-6 d, and then colonies were picked and used to inoculate a new BCDAT plate. After incubation for a further 15 to 16 d, colonies of WT or mutants were imaged with a commercially available digital camera (DMC-G2; Panasonic) on Olympus S2X12 microscope. However, iOX lines were only incubated for 8 d in a new BCDAT plate and then transfer and incubated on BCDAT medium supplemented with 1 μM β-estradiol (Sigma), or on BCDAT with 0.001 % dimethyl sulfoxide (DMSO) (Wako) as a control for 7 d. Then, gametophores were counted manually for each established colony by dissection.

3.2. Cell number and length observation

For the cell length measurement, protoplasts of WT or *ralf* mutans were cultured on PRM-B medium for two or three days under continuous light and then transferred to BCDAT medium supplemented with 0.5% glucose (BCDATG) and cultivated for 9 d under 0.5 μmol m^{-2} s^{-1} unilateral red light (λmax = 660± 20 nm). Unilateral red light was produced by passing light, provided by 40-W white fluorescence tubes (FLR40S-EX-N/M/36; Mitsubishi), through a 3-mm-thick red plastic filter (No. 102; Mitsubishi) into light-proof boxes. In contrast, iOX lines

were transferred on BCDATG supplemented with 1 μM β-estradiol (Sigma), or on BCDAT with 0.001% dimethyl sulfoxide (DMSO) (Wako) as a control for seven days under unilateral red light (red plastic filter (No. 102; Mitsubishi)), and imaged by Leica DMLB microscope as explained as follows.

3.3. Microscopic observation and statistical analysis

For bright field observation, chloronemal cells of wild-type, knock-out mutants and iOX lines were observed and imaged with a Leica DMLB microscope equipped with a CoolSNAP Color digital camera (Nippon Roper). The moss colonies were observed and imaged under the stereomicroscope (Olympus S2X12) and images were captured using a commercial digital camera (Panasonic Lumix DML-G2). Fiji (Image J) (https://imagej.net/software/fiji/) software was used to score subapical cell length, cell number and colony size. Average (mean), standard deviation (SD) and either t-test or ANOVA with post-hoc test according to Tukey were used with P-values <0.01, as indicated.

3.4. Immunoblotting

Proteins were extracted from the protonemata by urea extraction buffer (4 M urea (Sigma), 100 mM DTT (Wako), 1% Triton X-100, proteinase inhibitor (cOmplete Mini, EDTA-free, Sigma-Aldrich). The homogenate was spun down for 5 mins at 20,000 *g* to remove cell debris. The protein extract was mixed with protein loading buffer and heated at 68ºC for 5 minutes. I used mouse monoclonal anti-GFP JL-8 (Clontech, dilution 1:1,000) to detect PpRALF1-Citrine and PpRALF2-Citrine at room temperature for 2 hours. Secondary antibody used was anti-mouse HRP antibody (Amersham ECL Mouse IgG, dilution 1:5000) at room

temperature for 1 hour. Protein bands were visualized with ECL plus (Amersham ECL Prime Western Blotting Detection Reagent, GE Healthcare) used for chemiluminescent detection reagent and photographed using the LAS-3000 system (Fujifilm LAS-3000 imager).

4. Result

4.1. Disruption of PpRALF1 and PpRALF2 in *P.patens* impairs protonemal development

A BLAST search using the *A. thaliana* RALF1 (AtRALF1) amino acid sequence as a query against the *P. patens* genome (Phytozome v13, v3.0 assembly) revealed three putative RALF homologs: *PpRALF1* (gene identifier Pp3c3_15280), *PpRALF2* (gene identifier Pp3c6_7200) and *PpRALF3*, (gene identifier Pp3c25_4180).

To investigate a role of RALF in moss development of *P. patens,* I generated *ralf* knock-out mutants in various combinations: *Ppralf1*, *Ppralf2*, *Ppralf3, ralf2dko*, *Ppralf2,3dko* and *Ppralf1,2,3tko* (Table S2). Since mutant of the AtRALF34 showed a phenotype related to the planar cell polarity (PCP) of lateral root of *A. thaliana* (Murphy et al., 2016), I checked the phenotype of *Ppralf* mutants in relation to protonematal branching pattern in *P. patens*. However, I could not detect any deviation from the branching pattern in all *Ppralf* mutants (Fig. 1). Interestingly, I found some of the mutants showed unusual smooth edge on the colonies (Figure 2). This "smooth-edge colony" phenotype was visible in colonies regenerated from single protoplasts in single (*Ppralf1* and *Ppralf2*), double (*Ppralf1,2dko* and *Ppralf2,3dko*), and triple (*Ppralf1,2,3tko*) *ralf* knock-out mutants (Figure 2). The smooth edge phenotype was observed after 20 days of incubation on BCDAT medium. However, this smooth-edge phenotype was not observed in the *Ppralf*3 lines. Then, when checked this smooth-edge feature in *Ppralf1* mutant under microscope, I found that this smooth edge feature is dominated by chloronemata cells and

is opposite to the hairy/rough protonematal edge in wild type that is dominated by caulonemata (Figure S1).

As development progresses, or in response to certain environmental cues, dividing chloronemal cells may undergo transition to give rise to the more elongated caulonemal cells. In addition, modified protonemal side branches also give rise to buds, which in turn develop into leafy gametophores. I, therefore, checked the *Ppralf* mutants during gametophore production as it represents the downstream of cell fate transition/differentiation from choronema to caulonema. The result showed that in every mutant, except *Ppralf3* (mean = 23.33 ± 9.86), gametophore production was reduced significantly in *Ppralf1* (mean= 6.33 ± 3.53), *Ppralf2* (mean= 2 ± 1.73) , *Ppralf1,2dko* (mean = 0.78 ± 0.92), *Ppralf2,3dko* (mean = 1.88 ± 2.20) and *Ppralf1,2,3tko* (mean = 1.33 ± 1.66) when compared to WT (mean = 32.06 ± 10.67) after 20 days of incubation on BCDAT medium (Figure 3). Only the *Ppralf3* mutant was similar to WT in producing gametophores with the hairy protonematal edge. On the other hand, I also found that smooth-edge phenotype in the *Ppralf1,3dko* (Figure 2), indicating that PpRALF1 disruption is responsible for the mutant phenotype. Therefore I continued to focus on characterizing *PpRALF1* and *PpRALF2*. Extended incubation (30 days) on WT against *Ppralf1*, *Ppralf2*, and *Ppralf1,2dko* showed the same result on number gametophores (Figure S2). This extended incubation result suggested that the phenotype cannot be simply explained by delayed gametophore development in these mutants. Rather, I think that *Ppralf1*, *Ppralf2*, and *Ppralf1,2dko* might be having less gametophores production than wild-type as the consensus of fewer caulonemal cells number as precursor of gametophores.

To support my data, I conducted a more detailed analysis on the choloronema-to-caulonema differentiation in *Ppralf1*, *Ppralf2* and *Ppralf1,2dko* by quantifying the proportion of

chloronema and caulonemata in a colony. Indeed, the proportion of caulonemata was drastically reduced in the *Ppralf1, Ppralf2* and *Ppralf1,2dko* mutants (Figure 4), consistent with the reduced gametophore phenotype. Thus, I concluded that the "smooth-edge" and reduced gametophore phenotypes in *Ppralf1*, *Ppralf2,* and *Ppralf1,2dko* were consequences of decreased caulonemata formation. Then, based on these phenotype observations, PpRALF1 and PpRALF2 may play an essential role on protonemal development.

4.2. Disruption of PpRALF1 or PpRALF2 reduces cell length and cell number in chloronema cells

As the *Ppralf* mutant lines have smooth-edge colonies due to delayed cell fate transition, next I investigated whether the chloronemata has any delayed growth. Menand et al. (2007) reported that in *P. patens* both chloronemal and caulonemal cells elongate by a form of tip growth as a mode of cell growth. The chloronema cells elongate at the rate of 5.8±60.51μm h^{-1}, and gradually these chloronema will differentiate into caulonema cells that elongate at 19.87±2.18 μm h^{-1} (Menand et al., 2007). Smooth edge and reduced gametophores numbers in *Ppralf1*, *Ppralf2,* and *Ppralf1,2dko* may be due to impairment in chloronemata cell growth/elongation. I first tested the chloronemal cell growth in *Ppralf* mutants during protoplast regeneration under white light, but no discernible phenotype was visible (Figure 1). However under unilateral red light condition in which the side branch initiation is inhibited (Aoyama et al., 2012), the length of chloronema cells in *Ppralf1,2dko* was severely impaired in the sub apical cells (Figure 5a,b). The sub-apical cell was chosen for cell length quantification because this cell has fully elongated. The observation showed a significant reduction in cell length in *Ppralf1* (mean= 68.88 μm ± 7.70 μm), *Ppralf2* (mean= 69.79 μm ± 10.02 μm), and *Ppralf1,2 dko* (mean= 66.38 μm ± 10.14 μm) when compared to the WT (mean= 96.56 μm ± 13.17 μm) (Fig.

5c). From this experiment, I found that cell length reduced significantly to 30% in *Ppralf1*, *Ppralf2* and *Ppralf1,2dko*. This indicates that PpRALF1 and PpRALF2 loss-of-function reduced the cell length in chloronemata cells.

I also observed a phenotype in the cell number. In principle, reducing cell length may delay the cell cycle progression and it may lead to a lower cell number. One of the RALF functions is controlling cell cycle division (Gonneau et al., 2018). Expectedly, the cell number of chloronemal filaments was also reduced in the *Ppralf1* (mean= 8.23 ± 1.31), *Ppralf2* (mean= 7.98 ± 1.36) and *Ppralf1,2dko* (mean= 6.3µm ± 2.08) when compared to WT (mean= 16.2 ± 2.67) (Fig. 5d). From this phenotypic characterization, we conclude that the PpRALF1 and PpRALF2 are important for the protonemata growth in which the cell length and cell number of filamentous protonemata are dependent on PpRALF1 or PpRALF2.

4.3. Overexpression of PpRALF1 and PpRALF2 impaired chloronemal cell length and highlighted their overlapping roles in chloronema tip growth.

Since I found several compromised phenotypes in the protonemata growth, cell length and cell number, I hypothesized that the primary role of PpRALF1 and PpRALF2 might be involved in promoting protonemata growth. To test my hypothesis, I examined protonemata growth in weak and strong overexpressors for PpRALF1 and PpRALF2 C-terminal Citrine-fusion reporter lines. These overexpressor lines are beta-estradiol inducible lines. Expression levels of the strong iOX:PpRALF1-Citrine line (#1), weak iOX:PpRALF1-Citrine line (#2), strong iOX:PpRALF2-Citrine line (#17) and weak iOX:PpRALF2-Citrine line (#22) have been checked by GFP immunoblotting .

Interestingly, I found that the strong iOX:PpRALF1-Citrine showed shortened chloronemata cell length (DMSO: 91.45 µm ± 11.01 µm; 1 μM β-Est: 57.56 µm ± 9.39 µm) after

7 days incubation under red light condition (Fig. 6 a, b, e). This phenotype is similar to the *Ppralf1* and *Ppralf1,2 dko* under the red light condition. Subsequently, the shortened chloronemata cell directly led to a fewer cell number (DMSO: 8.89 ± 1.14; 1 μM β-Est: 6 ± 0.83, Fig. 6f) as well. As expected, the strong iOX:PpRALF1-Citrine line also exhibited "smooth-edge" colony phenotype when incubated on BCDAT supplemented with 1 μM β-Est (Fig. 7b). When I observed the colony size and number of gametophore, I found that strong overexpression of iOX:PpRALF1-Citrine significantly reduced the colony size (DMSO: 39.96 µm ± 5.51 µm; 1 μM β-Est: 25.98 µm ± 1.97 µm, Fig. 7e) as well as the gametophore number (DMSO: 18.4 ± 8.26; 1 μM β-Est: 2.3 ± 0.46, Fig. 7f). In contrast, weak overexpression of the iOX:PpRALF1-Citrine showed only a mild impact on the cell length (DMSO: 81.15 µm ± 10.34 µm; 1 μM β-Est: 71.64 µm ± 9.43 µm, Fig. 6c, d, e), and cell number (DMSO: 9.06 ± 1.46; 1 μM β-Est: 8.41 ± 1.52, Fig. 6f). I also found that the weak iOX:PpRALF1-Citrine overexpressor showed a mild impact on colony size (DMSO: 49.85 µm ± 6.21 µm; 1 μM β-Est: 42.39 µm ± 6.73 µm, Fig. 7e). Furthermore, colonies of the weak iOX:PpRALF1-Citrine overexpressor have rough edge/hairy phenotype on either DMSO or 1 μM β-Est-supplemented medium (Fig 7c, 7d). For the gametophore number, I also observed no significant difference in the weak iOX:PpRALF1-Citrine overexpressor (Fig. 7f). Therefore, the iOX:PpRALF1-Citrine lines exhibited a dosage-dependent response in cell length and cell division during chloronema tip growth.

Next, I also conducted phenotypic analyses using strong iOX:PpRALF2-Citrine line (#17) and weak iOX:PpRALF2-Citrine line (#22) overexpressors (Fig. 8). In general, I found the iOX:PpRALF2-Citrine overexpressor has a similar phenotype like that in the iOX:PpRALF1-Citrine overexpressor. In details, phenotype of the strong iOX:PpRALF2-Citrine overexpressor has short sub apical cells (DMSO: 83.35 µm ± 9.82 µm; 1 μM β-Est: 54.24 µm ± 8.34 µm, Fig. 8

a, b, e) and a reduced cell number (DMSO: 8.85 ± 1.19; 1 μM β-Est: 4.98 ± 1.07, Fig. 8f) in chloronemal filaments under red light condition. Furthermore, I also checked the phenotype of the strong iOX:PpRALF2-Citrine overexpressor and observed a "smooth-edge colony" phenotype (Fig. 9a, b). Moreover, colony size (DMSO: 37.62 µm ± 5.76 µm; 1 μM β-Est: 20.98 µm ± 2.98 µm, Fig. 9e) and gametophore number (DMSO: 18.4 ± 8.26; 1 μM β-Est: 2.3 ± 0.46, Fig. 9f) of the strong iOX:PpRALF2-Citrine overexpressor was reduced significantly after β-estradiol treatment.

Next I characterized the weak iOX:PpRALF2-Citrine overexpressor. Similar to the weak iOX:PpRALF1-Citrine overexpressor, iOX:PpRALF2-Citrine line (#22) exhibited a mild impact in chloronema subapical cell length (DMSO: 87.32 µm ± 11.94 µm; 1 μM β-Est: 77.37 µm ± 11.72 µm, Fig. 8 c,d, e), and cell number (DMSO: 9.06 ± 1.46; 1 μM β-Est: 8.42 ± 1.52, Fig. 8f) under red light condition. Indeed, this weak iOX:PpRALF2-Citrine overexpressor has a similar colony size before and after induction (DMSO: 49.87 µm ± 5.46 µm or 1 μM β-Est: 46.70 µm ± 5.94 µm, Fig. 9 c, d, e). Furthermore, I also found that the number of gametophores in the weak iOX:PpRALF2-Citrine overexpressor was reduce to half (DMSO: 14.2 ± 5; 1 μM β-Est: 7.67± 3.26, Fig. 9 f) in which the gametophores number of strong iOX:PpRALF2-Citrine line (#17) was completely inhibited (DMSO: 7 ± 2.51; 1 μM β-Est: 0, Fig. 9 f). This phenomenon was consistent with the previous result in which the number of gametophore in *Ppralf2* (2 ± 1.73) was significantly reduced compared to *Ppralf1* (6.33 ± 3.54) and WT (32.06 ± 10.67) (Fig. 3). PpRALF2 may have a role in regulating gametophore formation.

In conclusion, phenotypic characterization of the PpRALF1 and PpRALF2 overexpressor reveals the dosage effects of PpRALF1 and PpRALF2 expression level. In addition, the growth

defects observed in PpRALF1 and PpRALF2 overexpressor and knock-out mutants highlighted their overlapping roles in chloronemal growth.

4.4. PpRALF1 and PpRALF2 displayed different localization demonstrating their involvement in facilitating protonema tip growth.

To investigate the subcellular localization of PpRALF1 and PpRALF2 proteins, in-frame knock in reporter lines of PpRALF1-Citrine and PpRALF2-tagRFP was generated (unpublished materials kindly provided from Dr. Ooi-kock Teh). Here, PpRALF1-Citrine and PpRALF2-tagRFP were expressed under their native promoters. Subcellular localization of PpRALF1-Citrine was detected to localise evenly on the plasma membrane (Fig.10a) and PpRALF2-tagRFP accumulated polarly at the tip of apical cells (arrowhead, Fig. 10b). Even though PpRALF1 and PpRALF2 displayed different localization, this result suggested that PpRALF1 and PpRALF2 play a role in promoting chloronema elongation using different modes of actions.

Next, to understand whether the apical localization of PpRALF2-tagRFP has any correlation with the chloronemata apical growth, I tried to track the signal of PpRALF2-tagRFP in the apical cells. Here, I observed the protoplast regeneration process which shows apical tip growth. Observation of protoplasts from different regeneration stages showed that in intact protoplast the PpRALF2-tagRFP localized evenly on the plasma membrane (Fig 10 c, d). After protrusion happened, we found that the PpRALF2-tagRFP signal accumulated at the protrusion site. This indicated that the PpRALF2-tagRFP signal clearly arose around apical tip growth. Indeed, the signal of PpRALF2-tagRFP persisted throughout the tip growth until the first asymmetric division was completed (Fig. 10 e-j). Finally, the subcellular localization of the PpRALF1 and PpRALF2 suggested that they are involved in protonemata tip growth.

4.5. Proteolytic cleavage of PpRALF1 is necessary for its function

In Arabidopsis, the primary structure of some RALF precursors contain a conserved dibasic motif RRXL motif which is upstream to the active peptide and suggest that RALF precursors undergo proteolytic processing. Recent studies have shown that this site is required for the pro-peptide processing and activities of both AtRALF1 (Matos et al., 2008) and AtRALF23 (Srivastava et al., 2009). Overexpression of a preproAtRALF1 causes semi-dwarfism whereas overexpression of a preproAtRALF1(R69A) that contains a mutated dibasic site exhibited normal growth. This indicated that proteolytic processing of RALFs is important for its function (Matos et al., 2008; Srivastava et al., 2009). Srivastava et al (2009) has identified AtS1P as the protease that is required for the processing of AtRALF23.

Although both PpRALF1 and PpRALF2 are genetically required for protonema cell elongation, they are structurally distinguishable by the presence of an S1P cleavage site, RRLL motif, in the PpRALF1 (Fig.11a). Previously it reported that a dibasic site upstream of a plant peptide hormone, AtRALF1 and AtRALF23, is essential for processing. AtRALF peptides are expressed as precursors that need to be cleaved by S1P in order to produce a mature RALF peptide that can execute its function (Matos et al., 2008; Srivastava et al., 2009) . Therefore I next wanted to investigate if PpRALF1 is also proteolytically processed *in vivo* and how this cleavage may affect its function by replacing one of the basic amino acids, Arginine, to Alanine (R73A, Fig. 11a). The iOX:PpRALF1^{R73A}-Citrine was expressed as an inducible construct (unpublished materials from Dr. Ooi-kock Teh) in *P.patens*. After screening of all the available transgenic lines using GFP-immunoblot, I obtained an expressing transgenic line, iOX:PpRALF1^{R73A}-Citrine line (#6). Western blot analyses revealed that the PpRALF1-Citrine (predicted MW = 43.7kDa) migrated in two forms: the unprocessed proPpRALF1 and the

cleaved mature mPpRALF1. The mPpRALF1 migrated faster than the proPpRALF1 (predicted MW = 40 kDa) (Fig. 11b). However, the PpRALF1^{R73A}-Citrine transgenic line only produced a non-cleaved form (Fig. 11b), suggesting that the monobasic site is no longer efficiently processed by proteases. Next, I conducted morphological characterization on the iOX:PpRALF1 ^{R73A} –Citrine line and it exhibited normal chloronemata subapical cell length (DMSO: 100.29 µm ± 8.75 µm; 1 μM β-Est: 99.77 µm ± 8.50 µm, Fig. 11d) and cell number (DMSO: 9.43 µm ± 1.12 µm; 1 μM β-Est: 9.38 µm ± 1.03 µm Fig. 11e) after beta-estradiol induction under the red light conditions. Indeed, when we incubated iOX:PpRALF1^{R73A}-Citrine on BCDAT supplemented with 1μM β-estradiol under white light condition, there was no difference in the appearance of colony edge (Fig. 11g) and gametophores numbers (Fig. 11f). Therefore, I conclude that the PpRALF1 is cleaved *in vivo* at the S1P cleavage site and this process affects the PpRALF1 function.

5. Discussion

It is well known that RALFs function in many plant species and have been known to act as negative regulators of plant growth. In Arabidopsis, the AtRALF1 peptide has been well-characterized and known to inhibit cell elongation of the primary root (Haruta et al., 2014). Cell elongation appears to be primary mechanisms that the RALF family affects, as seen through synthetic peptide application and overexpression (Murphy & De Smet, 2014; Pearce et al., 2001). Not only as a negative regulator, recently RALF also has been shown to play a positive role in regulating root hair tip growth (Zhu et al., 2020).

In my research, interestingly I found that PpRALF1 and PpRALF2 showed an overlapping function in promoting protonemata tip growth. Based on knock out phenotype, I

hypothesized that PpRALF1 and PpRALF2 might form a heterodimer before binding to a receptor and induce downstream signalling that is necessary to promote tip growth. The recent report of the cysteine-rich transmembrane module (CYSTM) members, as the non-secreted cysteine-rich peptides (NCRPs), showed that between signaling peptide may be involved in cellular signaling by forming homodimers or heterodimers to activate the stress-related signaling pathway (Xu et al., 2018).

The function of PpRALF1 and PpRALF2 in promoting protonemata tip growth is also similar to the AtRALF1 in regulating in root hair tip growth. Zhu et al (2020) reported that to promote root hair polar growth, the RALF1–FER complex promotes the mRNA translation of root hair-specific genes, including RSL4 and ROP2, by facilitating eIF4E1 phosphorylation. The root hairs emerge from the primary root as tip-growing structures which are similar to the tip growth exhibited by chloronemata and caulonemata in moss (Menand et al., 2007). Therefore, I think that promotion of protonema tip growth by the PpRALF1 and PpRALF2 may have similar mechanisms as the AtRALF1 in promoting root hair tip growth. Thus, it is likely that tip growth-promoting function of RALF is conserved between bryophytes and vascular plants.

It is interesting to note that the iOX:RALF1-Citrine and iOX:RALF2-Citrine overexpressors phenocopied the loss-of-function alleles by exhibiting inhibition of protonemata growth. Although I expected that overexpressors display enhanced tip growth as adding exogenous treatment of synthetic AtRALF1 showed in elongation phases of root hair growth (Zhu et al., 2020), it is not unusual that hypermorphic and loss-of-function alleles exhibit a similar phenotype such as the hypermorphic allele the 35S::RALF34 overexpression lines (Gonneau et al., 2018) and RALF34 loss-of-function alleles (Gonneau et al., 2018; Murphy et al., 2016). This indicates that the dosage-dependent regulation of RALF activity is critical for normal

signaling pathway in these contexts as reported by Gonneau et al (2018). Another possibility to explain for this phenomenon is that PpRALF overexpression enforces a titration effect which dilutes out the receptor activation responses. Therefore, overexpressed peptides made the tip growth dysfunctional.

The PpRALF1 and PpRALF2 have different localizations in which PpRALF1 symmetrically localised on the plasma membrane while PpRALF2 accumulated at the growing tip. Interestingly, the apical localization of PpRALF2 is similar to that of AtRALF1 (Zhu et al., 2020). Different localization between the PpRALF1and PpRALF2 may indicate cooperative roles between PpRALF1 and PpRALF2 in tip growth promotion, possibly through activating receptors that are mechanistically similar to the AtRALF1 during root hair tip growth promotion. According to the GenBank and Phytozome, the CrRLK1L protein kinase subfamily to which FERONIA receptor kinase belongs is present in *P. patens* (Galindo-trigo et al., 2016), implying that a signaling pathway of RALF and its receptor in *A. thaliana* is present in *P. patens*.

Finally, my study demonstrated that only the PpRALF1 has an RRLL motif. The pair of Arg residues (RR), a feature typically found in animal prohormones processed by convertases, is located just upstream from the N terminus of the active peptide in almost all RALFs (Pearce et al., 2001). Moreover, Matos et al. (2008) reported that a canonical subtilase site (also characterised by a dibasic RR motif) upstream from the presumed start of the mature peptide was important for the processing of the precursor of AtRALF1. Mutation in the second Arg residue demonstrated that the precursor was not processed, and the construct did not produce the overexpressor phenotype (Matos et al., 2008). Consistently, my results also showed that the PpRALF1 is proteolytically cleaved *in vivo* and this is necessary for the PpRALF1 function in tip growth.

6. Conclusion

My study reveals that PpRALF1 and PpRALF2 have overlapping functions in promoting protonema tip growth and elongation in *P.patens*, showing homologous function as the Arabidopsis RALF1 in promoting root hair tip growth, and proteolytic cleavage of PpRALF1 is necessary for its function.

7. Reference

Abarca, A., Franck, C. M., & Zipfel, C. (2021). Family-wide evaluation of rapid alkalinization factor peptides. *Plant Physiology*, *187*(2), 996–1010. https://doi.org/10.1093/plphys/kiab308

Aoyama, T., Hiwatashi, Y., Shigyo, M., Kofuji, R., Kubo, M., Ito, M., & Hasebe, M. (2012). AP2-type transcription factors determine stem cell identity in the moss *Physcomitrella patens*. *Development (Cambridge)*, *139*(17), 3120–3129. https://doi.org/10.1242/dev.076091

Ashton, N. W., & Cove, D. J. (1977). The isolation and preliminary characterisation of auxotrophic and analogue resistant mutants of the moss, *Physcomitrella patens*. *MGG Molecular & General Genetics*, *154*(1), 87–95. https://doi.org/10.1007/BF00265581

Campbell, L., & Turner, S. R. (2017). A comprehensive analysis of RALF proteins in green plants suggests there are two distinct functional groups. *Frontiers in Plant Science*, *8*(January), 1–14. https://doi.org/10.3389/fpls.2017.00037

Cao, J., & Shi, F. (2012). Evolution of the RALF gene family in plants: Gene duplication and selection patterns. *Evolutionary Bioinformatics*, *2012*(8), 271–292. https://doi.org/10.4137/EBO.S9652

Cove, D. (2005). The moss *Physcomitrella patens*. *Annual Review of Genetics*, *39*, 339–358. https://doi.org/10.1146/annurev.genet.39.073003.110214

Cove, D. J., Perroud, P. F., Charron, A. J., McDaniel, S. F., Khandelwal, A., & Quatrano, R. S. (2009). The moss *Physcomitrella patens*: A novel model system for plant development and genomic studies. *Cold Spring Harbor Protocols*, *4*(2). https://doi.org/10.1101/pdb.emo115

Covey, P. A., Subbaiah, C. C., Parsons, R. L., Pearce, G., Lay, F. T., Anderson, M. A., Ryan, C. A., & Bedinger, P. A. (2010). A pollen-specific RALF from tomato that regulates pollen tube elongation. *Plant Physiology*, *153*(2), 703–715. https://doi.org/10.1104/pp.110.155457

Czyzewicz, N., Yue, K., Beeckman, T., & De Smet, I. (2013). Message in a bottle: Small signalling peptide outputs during growth and development. *Journal of Experimental Botany*, *64*(17), 5281–5296. https://doi.org/10.1093/jxb/ert283

Fu, C., Donovan, W. P., Shikapwashya-hasser, O., Ye, X., & Cole, R. H. (2014). Hot fusion : An efficient

method to clone multiple DNA fragments as well as inverted repeats without ligase. *Lic*, 1–20. https://doi.org/10.1371/journal.pone.0115318

Galindo-trigo, S., Gray, J. E., Smith, L. M., & Smith, L. M. (2016). Conserved roles of CrRLK1L receptor-like kinases in cell expansion and reproduction from algae to angiosperms. *Front. Plant Sci.*, *7*(August), 1–10. https://doi.org/10.3389/fpls.2016.012697

Ginanjar, F.G., Teh, O.-K., & Fujita, T. 2021. Characterisation of Rapid Alkalinisation Factors (RAFLs) in *Physcomitrium patens* reveals functional conservation in tip growth. *New Phytologist*, under revision.

Gonneau, M., Desprez, T., Martin, M., Vernhettes, S., Smet, I. De, Doblas, G., Bacete, L., & Miart, F. (2018). Receptor kinase THESEUS1 is a Rapid Alkalinization Factor 34 receptor in *Arabidopsis, Current Biology*. 28(15). 2452–2458. https://doi.org/10.1016/j.cub.2018.05.075

Haruta, M., Sabat, G., Stecker, K., Minkoff, B. B., & Sussman, M. R. (2014). A peptide hormone and its receptor protein kinase regulate plant cell expansion. *Science*, *343*(6169), 408–411. https://doi.org/10.1126/science.1244454

Jang, G., & Dolan, L. (2011). Auxin promotes the transition from chloronema to caulonema in moss protonema by positively regulating PpRSL1and PpRSL2 in *Physcomitrella patens*. *New Phytologist*, *192*(2), 319–327. https://doi.org/10.1111/j.1469-8137.2011.03805.x

Kofuji, R., & Hasebe, M. (2014). Eight types of stem cells in the life cycle of the moss *Physcomitrella patens*. *Current Opinion in Plant Biology* .17(1). 13–21). https://doi.org/10.1016/j.pbi.2013.10.007

Matos, J. L., Fiori, C. S., Silva-Filho, M. C., & Moura, D. S. (2008). A conserved dibasic site is essential for correct processing of the peptide hormone AtRALF1 in *Arabidopsis thaliana*. *FEBS Letters*, *582*(23–24), 3343–3347. https://doi.org/10.1016/j.febslet.2008.08.025

Menand, B., Calder, G., & Dolan, L. (2007). Both chloronemal and caulonemal cells expand by tip growth in the moss *Physcomitrella patens*. *Journal of Experimental Botany*, *58*(7), 1843–1849. https://doi.org/10.1093/jxb/erm047

Murphy, E., & De Smet, I. (2014). Understanding the RALF family: A tale of many species. *Trends in*

Plant Science, *19*(10), 664–671. https://doi.org/10.1016/j.tplants.2014.06.005

Murphy, E., Smith, S., & Smet, I. De. (2012). Small signaling peptides in *Arabidopsis* development : How cells communicate over a short distance. *Plant cell*. *24*(8), 3198–3217. https://doi.org/10.1105/tpc.112.099010

Murphy, E., Vu, L. D., Broeck, L. Van Den, Lin, Z., Ramakrishna, P., Cotte, B. Van De, Gaudinier, A., Goh, T., Slane, D., Beeckman, T., Inzé, D., Brady, S. M., Fukaki, H., & Smet, I. De. (2016). RALFL34 regulates formative cell divisions in *Arabidopsis* pericycle during lateral root initiation. *Journal of Experimental Botany*. *67*(16), 4863–4875. https://doi.org/10.1093/jxb/erw281

Nishiyama, T., Hiwatashi, Y., Sakakibara, K., Kato, M., & Hasebe, M. (2000). Tagged mutagenesis and gene-trap in the moss, *Physcomitrella patens* by shuttle mutagenesis. *DNA Research*, *7*(1), 9–17. https://doi.org/10.1093/dnares/7.1.9

Oh, E., Seo, P. J., & Kim, J. (2018). Signaling Peptides and Receptors Coordinating Plant Root Development. *Trends in Plant Science*, *23*(4), 337–351. https://doi.org/10.1016/j.tplants.2017.12.007

Pearce, G., Moura, D. S., Stratmann, J., & Ryan, C. A. (2001). RALF, a 5-kDa ubiquitous polypeptide in plants, arrests root growth and development. *Proceedings of the National Academy of Sciences of the United States of America*, *98*(22), 12843–12847. https://doi.org/10.1073/pnas.201416998

Pearce, G., Yamaguchi, Y., Munske, G., & Ryan, C. A. (2010). Structure-activity studies of RALF, Rapid Alkalinization Factor, reveal an essential - YISY - motif. *Peptides*, *31*(11), 1973–1977. https://doi.org/10.1016/j.peptides.2010.08.012

Prigge, M. J., & Bezanilla, M. (2010). Evolutionary crossroads in developmental biology: *Physcomitrella patens*. *Development*, *137*(21), 3535–3543. https://doi.org/10.1242/dev.049023

Rensing, S. A., Lang, D., Zimmer, A. D., Terry, A., Salamov, A., Shapiro, H., Nishiyama, T., Perroud, P. F., Lindquist, E. A., Kamisugi, Y., Tanahashi, T., Sakakibara, K., Fujita, T., Oishi, K., Shin-I, T., Kuroki, Y., Toyoda, A., Suzuki, Y., Hashimoto, S. I., … Boore, J. L. (2008). The Physcomitrella genome reveals evolutionary insights into the conquest of land by plants. *Science*, *319*(5859), 64–69.

https://doi.org/10.1126/science.1150646

Sharma, A., Hussain, A., Mun, B. G., Imran, Q. M., Falak, N., Lee, S. U., Kim, J. Y., Hong, J. K., Loake, G. J., Ali, A., & Yun, B. W. (2016). Comprehensive analysis of plant rapid alkalization factor (RALF) genes. *Plant Physiology and Biochemistry*, *106* (January 2018), 82–90. https://doi.org/10.1016/j.plaphy.2016.03.037

Srivastava, R., Liu, J. X., Guo, H., Yin, Y., & Howell, S. H. (2009). Regulation and processing of a plant peptide hormone, AtRALF23, in *Arabidopsis*. *Plant Journal*, *59*(6), 930–939. https://doi.org/10.1111/j.1365-313X.2009.03926.x

Stegmann, M., Monaghan, J., Smakowska-Luzan, E., Rovenich, H., Lehner, A., Holton, N., Belkhadir, Y., & Zipfel, C. (2017). The receptor kinase FER is a RALF-regulated scaffold controlling plant immune signaling. *Science*, *355*(6322), 287–289. https://doi.org/10.1126/science.aal2541

Wu, J., Kurten, E. L., Monshausen, G., Hummel, G. M., Gilroy, S., & Baldwin, I. T. (2007). NaRALF, a peptide signal essential for the regulation of root hair tip apoplastic pH in *Nicotiana attenuata*, is required for root hair development and plant growth in native soils. *Plant Journal*, *52*(5), 877–890. https://doi.org/10.1111/j.1365-313X.2007.03289.x

Xu, Y., Yu, Z., Zhang, D., Huang, J., Wu, C., Yang, G., & Yan, K. (2018). CYSTM , a Novel Non-Secreted Cysteine-Rich Peptide Family , Involved in Environmental Stresses in *Arabidopsis*

Zhu, S., Estévez, J. M., Liao, H., Zhu, Y., Yang, T., Li, C., Wang, Y., Li, L., Liu, X., Pacheco, J. M., Guo, H., & Yu, F. (2020). The RALF1–FERONIA Complex Phosphorylates eIF4E1 to Promote Protein Synthesis and Polar Root Hair Growth. *Molecular Plant*, *13*(5), 698–716. https://doi.org/10.1016/j.molp.2019.12.014

8. Figures

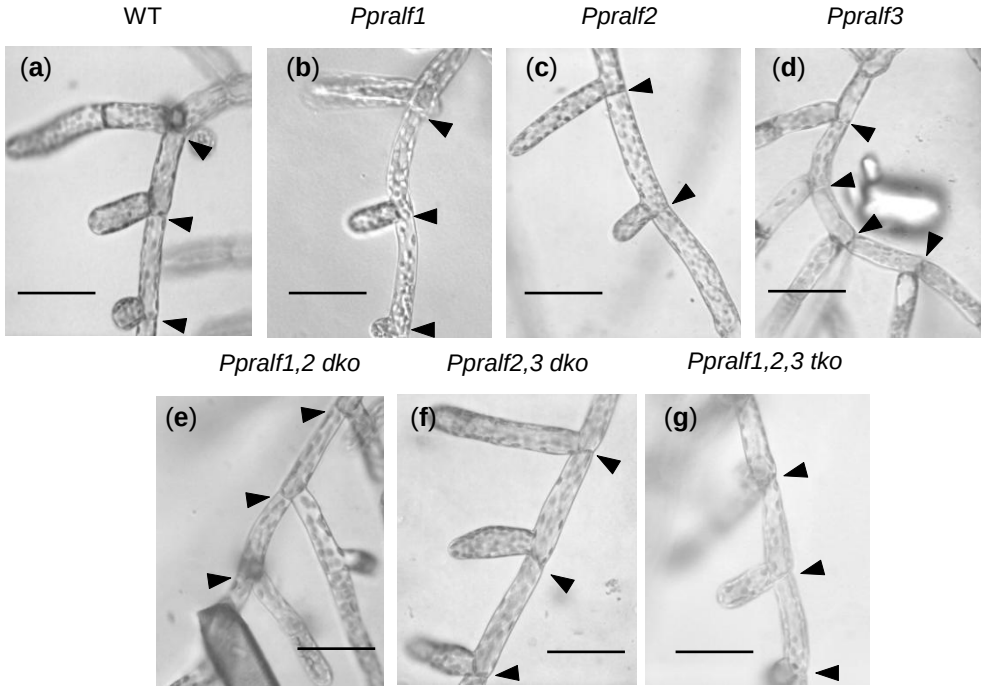

Figure. 1. *Ppralf mutants* show normal protonematal branch positioning under normal white light. Five-day-old protonema filaments of WT (a), *Ppralf1* (b), *Ppralf2* (c) *Ppralf3* (d), *Ppralf1,2 dko* (e), *Ppralf2,3 dko* (f) and *Ppralf1,2,3 tko* (g) regenerated from a protoplast on PRMT medium. Photos show from 4th to 7th cells number. Black arrowheads indicate septum. Bar: 0.5 mm.

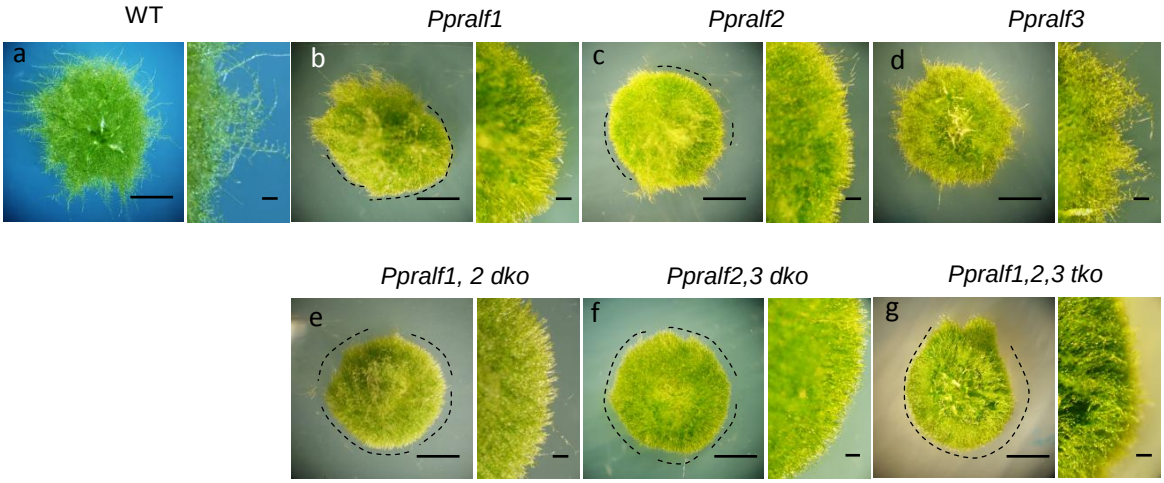

Figure. 2. *Ppralf* mutants show smooth edge colony except *Ppralf3*. (a-g) Growth phenotype of colonies of WT (a), *Ppralf1* (b), *Ppralf2* (c), *Ppralf3* (d), *Ppralf1,2 dko* (e), *Ppralf2,3 dko* (f) and *Ppralf1,2,3 tko* (g) which are regenerated from a protoplast on BCDAT medium for 20 days. Dash lines indicate smooth edge. Bars: 1 mm.

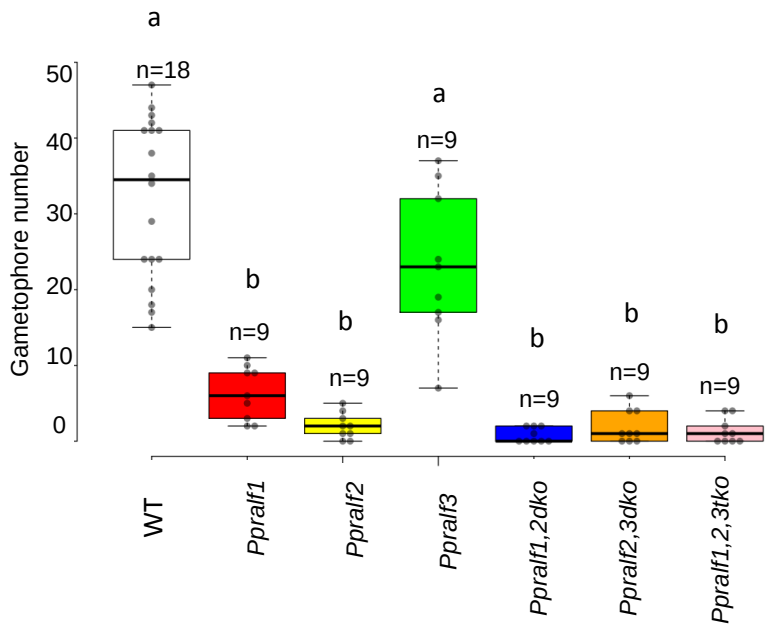

Figure. 3. Gametophore number of 20-day-old colonies of WT, *Ppralf1*, *Ppralf2*, *Ppralf3*, *Ppralf1,2 dko*, *Ppralf2,3 dko* and *Ppralf1,2,3 tko*. The box plot shows the number of gametophore/colony in WT (white box), *Ppralf1* (red blox), *Ppralf2* (yellow box), *Ppralf3* (green box), *Ppralf1,2 dko* (blue box), *Ppralf2,3 dko* (orange box) and *Ppralf1,2,3 tko* (pink box). The black horizontal line indicates the median value and the box represents the second and third quartiles. The upper and lower quartiles are represented as whiskers. Letters indicate statistically significant differences (one-way ANOVA and Tukey's post hoc test, $p < 0.01$). n= sample size.

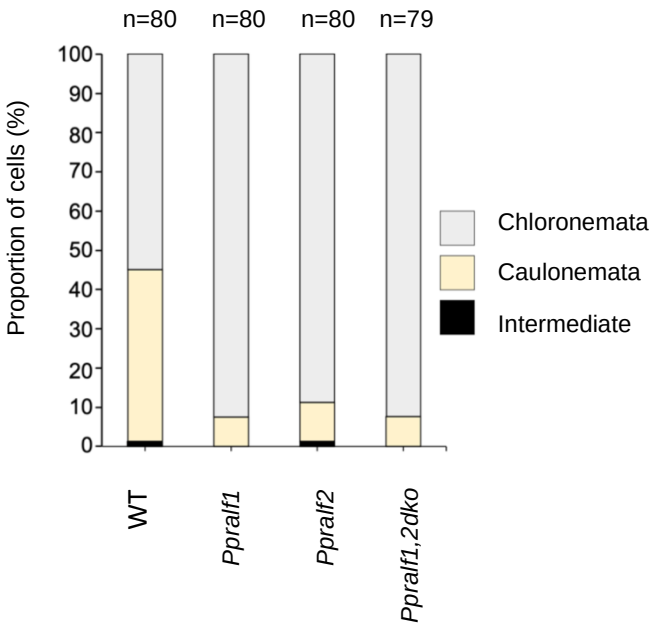

Figure. 4. Proportion of cells (%) of a colony of WT, *Ppralf1*, *Ppralf2*, and *Ppralf1,2 dko*. A stacked bar shows the proportion of chloronemal (grey), caulonemal (beige) and intermediate (black) cells in WT, *Ppralf1*, *Ppralf2* and *Ppralf1,2 dko*. n= sample size.

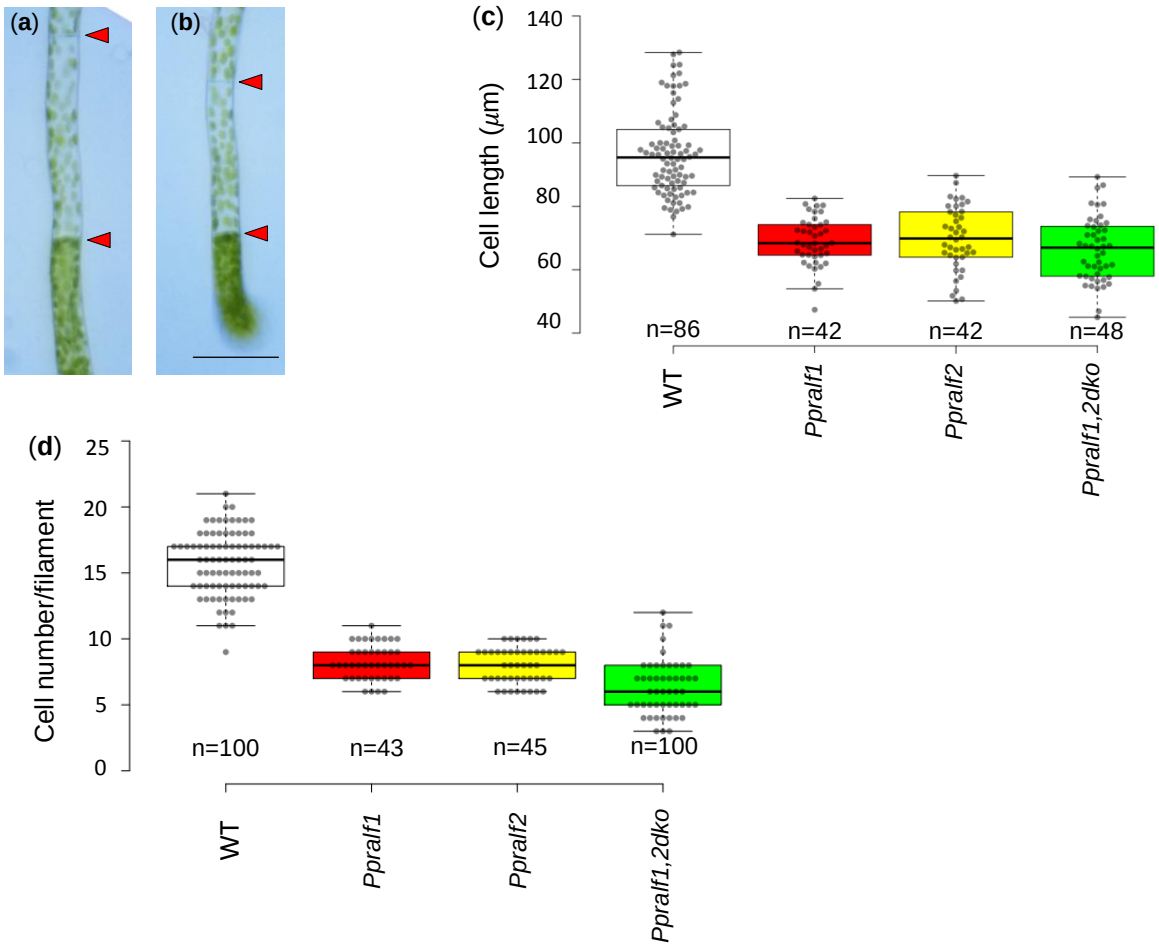

Figure. 5. Cell length inhibition of sub-apical cell and cell numbers in WT, *Ppralf1*, *Ppralf2*, and *Ppralf1,2* dko. Chloronemal filament of WT (**a**) and *Ppralf1,2 dko* (**b**) were grown in red-light condition. Red arrow heads indicate septum of the sub-apical cells. Bar: 50 μm. The box plot shows the cell length (**c**) and cell number (**d**) of WT (white box), *Ppralf1* (red blox), *Ppralf2* (yellow box), *Ppralf1,2 dko* (green box). The black horizontal line indicates the median value and the box represents the second and third quartiles. The upper and lower quartiles are represented as whiskers. Letters indicate statistically significant differences (one-way ANOVA and Tukey's post hoc test, $p < 0.01$). n= sample size.

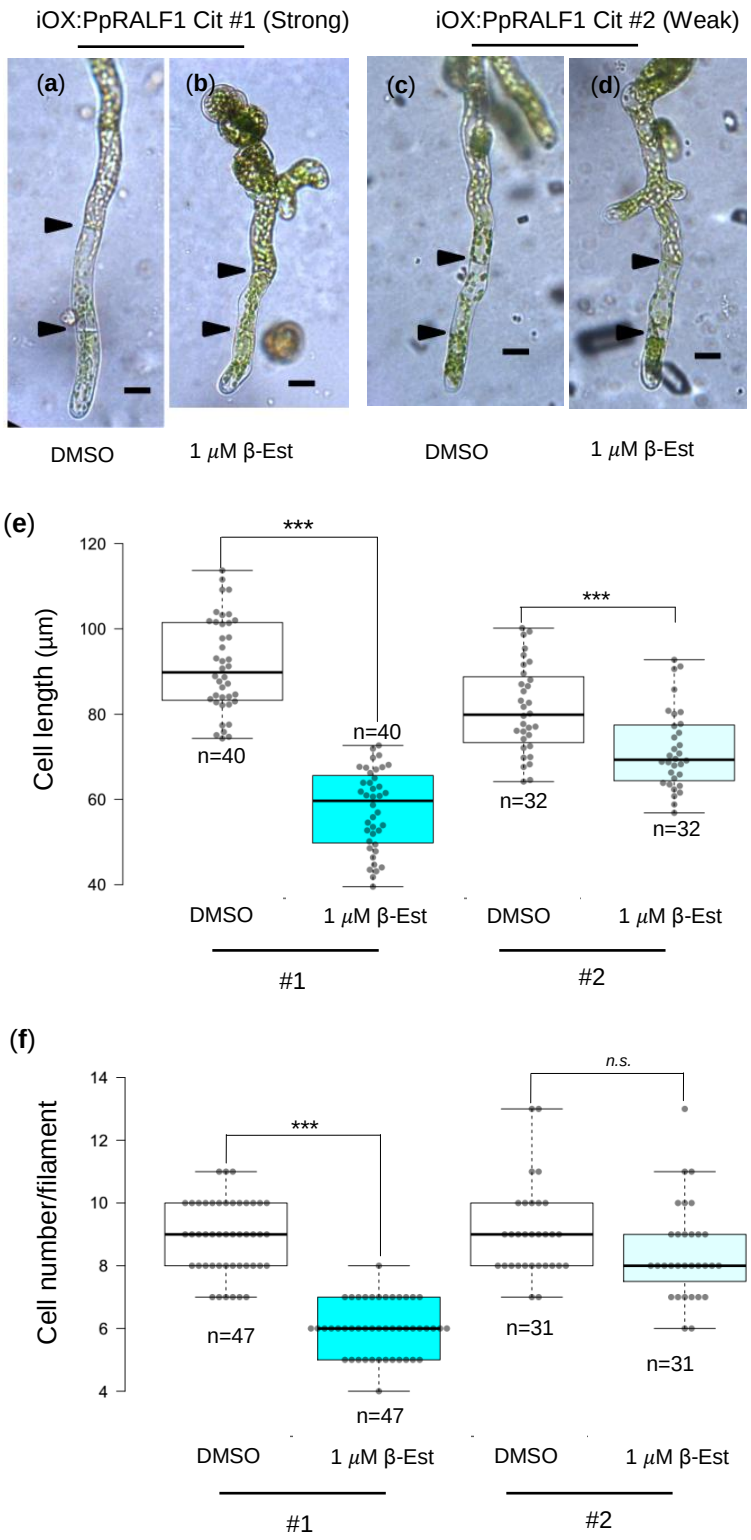

Figure 6. Overexpression of PpRALF1 impairs cell length and cell number (a-d). Protonemata of strong iOX:PpRALF1-Citrine line #1 (**a**, **b**) and weak iOX:Pp RALF1-Citrine line #2 (**c**, **d**). Chloronemata were grown under red light on either DMSO (**a**, **c**) or 1 μM **β**-estradiol (**b**, **d**) supplemented BCDAT medium for 7 days. Arrow heads indicate septums. Bars: 20 μm. The box plot shows the cell length (**e**) and cell number (**f**) of line #1

(white box: DMSO and cyan: 1 μM β-Est), and line #2 (white box: DMSO and light cyan: 1 μM β-Est). The black horizontal line indicates the median value and the box represents the second and third quartiles. The upper and lower quartiles are represented as whiskers. One-way ANOVA and Tukey's post hoc test were used to determine significant difference at $p < 0.01$ (indicated by ***) or not significant (*n. s.*). n=sample size.

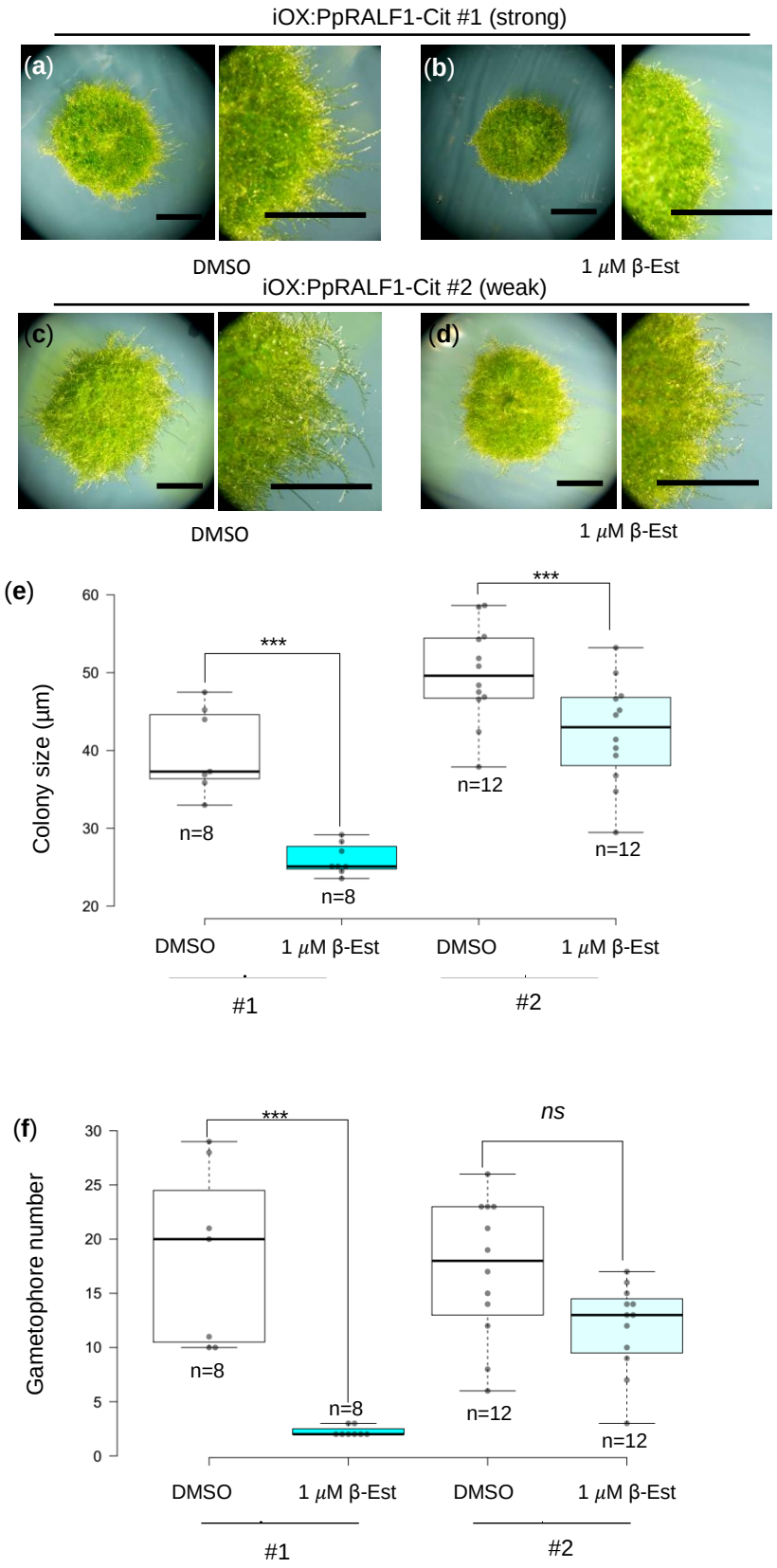

Fig.7. Overexpression of PpRALF1 impairs colony size and gametophore number. Colony phenotype (25-day-old) of strong iOX:PpRALF1-Citrine line#1 (**a**, **b**) and weak iOX:PpRALF1-Citrine line#2 (**c**, **d**). Colonies

were grown on BCDAT medium supplemented with either DMSO (**a**, **c**) or 1 μM **β**-estradiol (**b**, **d**). Bars: 3mm. (**e-f**) The box plot shows the colony size (**e**) and gametohore number (**f**) of line #1 (white box: DMSO and cyan: 1 μM β-Est), and line #2 (white box: DMSO and light cyan: 1 μM β-Est). The black horizontal line indicates the median value and the box represents the second and third quartiles. The upper and lower quartiles are represented as whiskers. One-way ANOVA and Tukey's post hoc test were used to determine significant difference at $p < 0.01$ (indicated by ***) or not significant (*n. s.*). n=sample size.

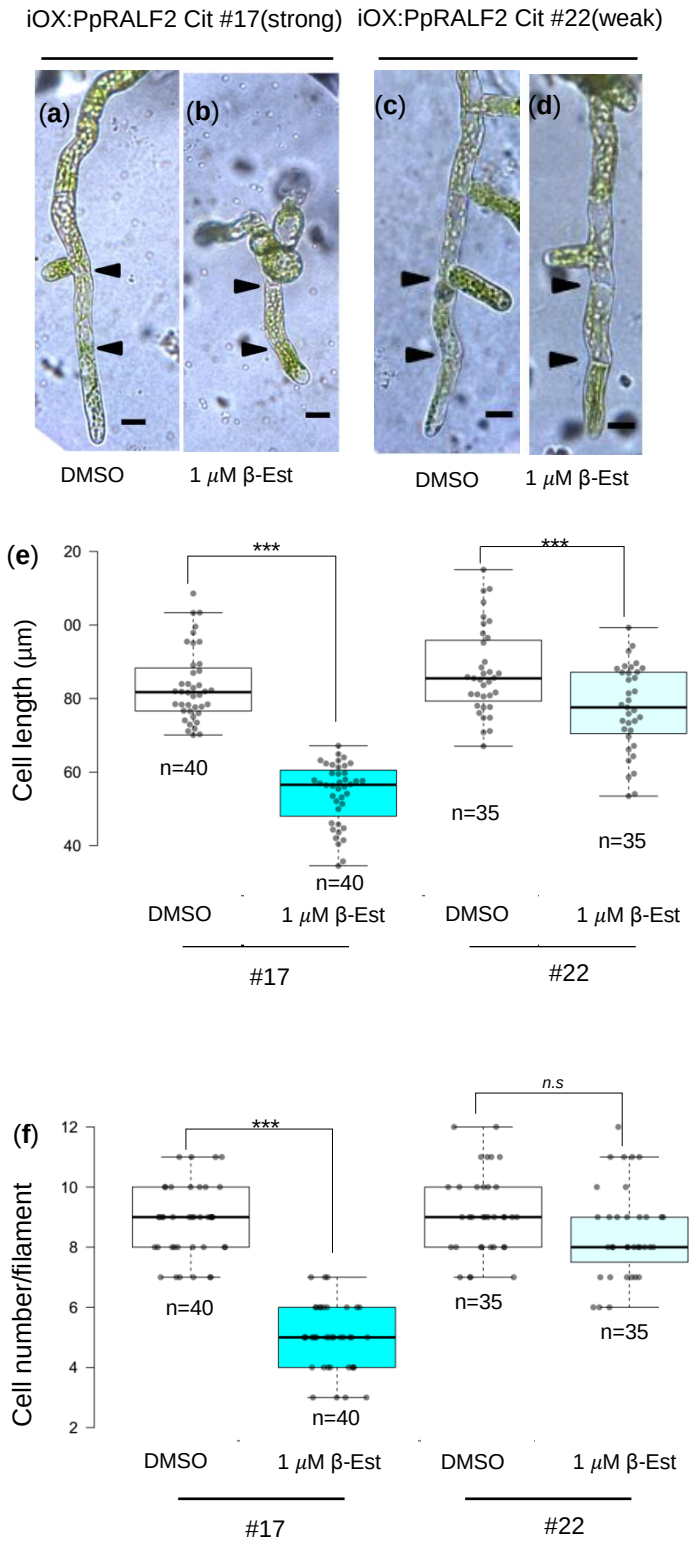

Fig. 8. Overexpression of PpRALF2 impairs cell length and cell number (**a-d**) Protonemata of strong iOX:PpRALF2-Citrine line#17 (**a**, **b**) and weak iOX:PpRALF2-Citrine line#22 (**c**, **d**). Chloronemata were grown under red light on either DMSO (**a**, **c**) or 1 μM **β**-estradiol (**b**, **d**) supplemented BCDAT medium for 7 days. Arrow

heads indicate septums. Bars: 20 μm. (**e-f**) The box plot shows the cell length (**e**) and cell number (**f**) of line #17 (white box: DMSO and cyan: 1 μM β-Est), and line #22 (white box: DMSO and light cyan: 1 μM β-Est). The black horizontal line indicates the median value and the box represents the second and third quartiles. The upper and lower quartiles are represented as whiskers. One-way ANOVA and Tukey's post hoc test were used to determine significant difference at $p < 0.01$ (indicated by ***) or not significant (*n. s.*). n=sample size.

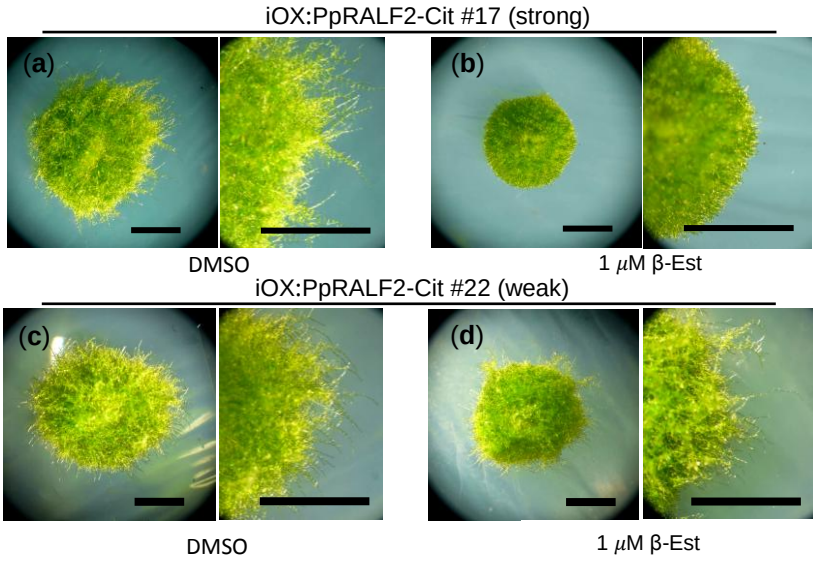
iOX:PpRALF2-Cit #17 (strong)
(a)
(b)
DMSO
1 μM β-Est
iOX:PpRALF2-Cit #22 (weak)
(c)
(d)
DMSO
1 μM β-Est

(**e**)

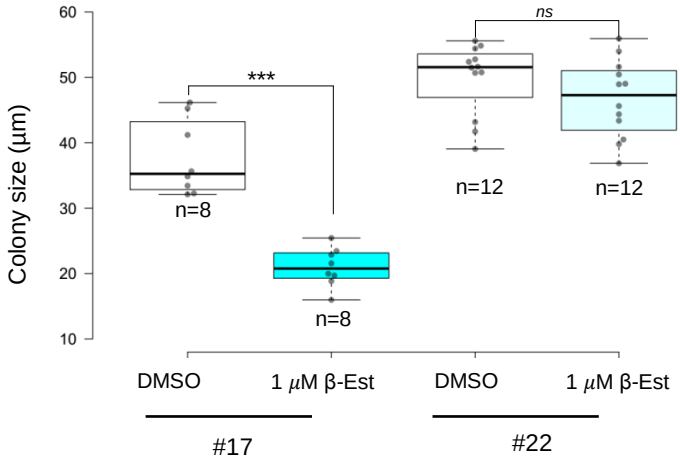
Colony size (μm)
60
50
40
30
20
10
***
ns
n=8
n=8
n=12
n=12
DMSO
1 μM β-Est
DMSO
1 μM β-Est
#17
#22

(**f**)

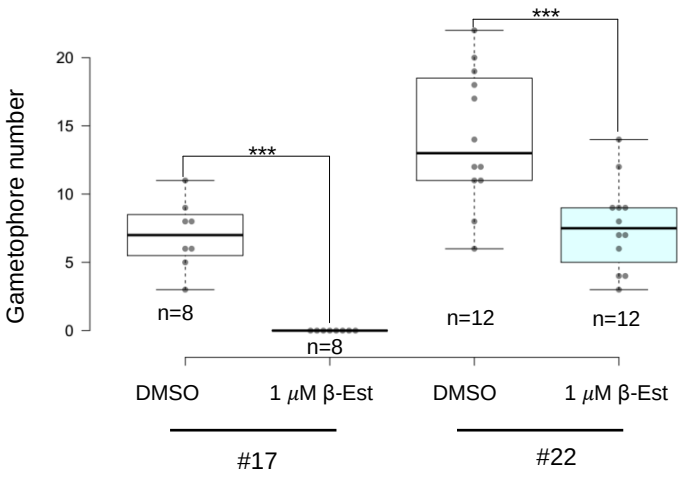
Gametophore number
20
15
10
5
0
***
***
n=8
n=8
n=12
n=12
DMSO
1 μM β-Est
DMSO
1 μM β-Est
#17
#22

Fig. 9. Overexpression of PpRALF2 impairs colony size and gametophores number (**a**-**d**). Colony phenotype (25-day-old) of strong iOX:PpRALF2-Citrine line#17 (**a**, **b**) and weak iOX:PpRALF2-Citrine line#22 (**c**, **d**). Colonies were grown on BCDAT medium supplemented with either DMSO (**a**, **c**) or 1 μM **β**-estradiol (**b**, **d**). Bars: 3mm. (**e**-**f**) The box plot shows the colony size (**e**) and gametophores number (**f**) of line #17 (white box: DMSO and cyan: 1 μM β-Est), and line #22 (white box: DMSO and light cyan: 1 μM β-Est). The black horizontal line indicates the median value and the box represents the second and third quartiles. The upper and lower quartiles are represented as whiskers. One-way ANOVA and Tukey's post hoc test were used to determine significant difference at $p < 0.01$ (indicated by ***) or not significant (*n. s.*). n=sample size.

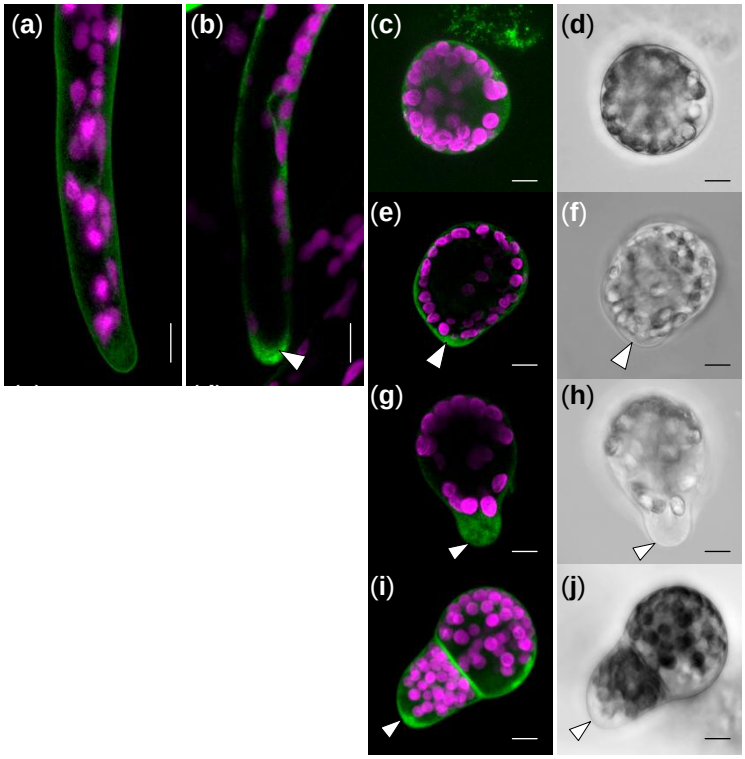

Figure 10. Subcellular localization is different between PpRALF1 and PpRALF2 during apical growth. (**a**-**d**) 5-day-old protonemata of PpRAFL1-Citrine (**a**) and PpRALF2-tagRFP (**b**) were grown on BCDAT. Confocal images shown are z-stack projections (sum), chloroplasts are indicated by magenta and green indicates Citrine (**a**). TagRFP is pseudocoloured as green for easier visualization (**b**). Apical accumulation of PpRALF2-tagRFP is pointed by an arrowhead. Bars= 10 µm. (**c**-**j**) Confocal images of regenerating protoplasts from PpRALF2-tagRFP. Fluorescent (**c**, **e**, **g**, **i**) and bright field (**d**, **f**, **h**, **j**) images shown are z-stack projections (sum). Chloroplasts are indicated by magenta and green indicates tagRFP. Arrowheads indicate apical accumulation of PpRALF2-tagRFP. Bars= 10µm.

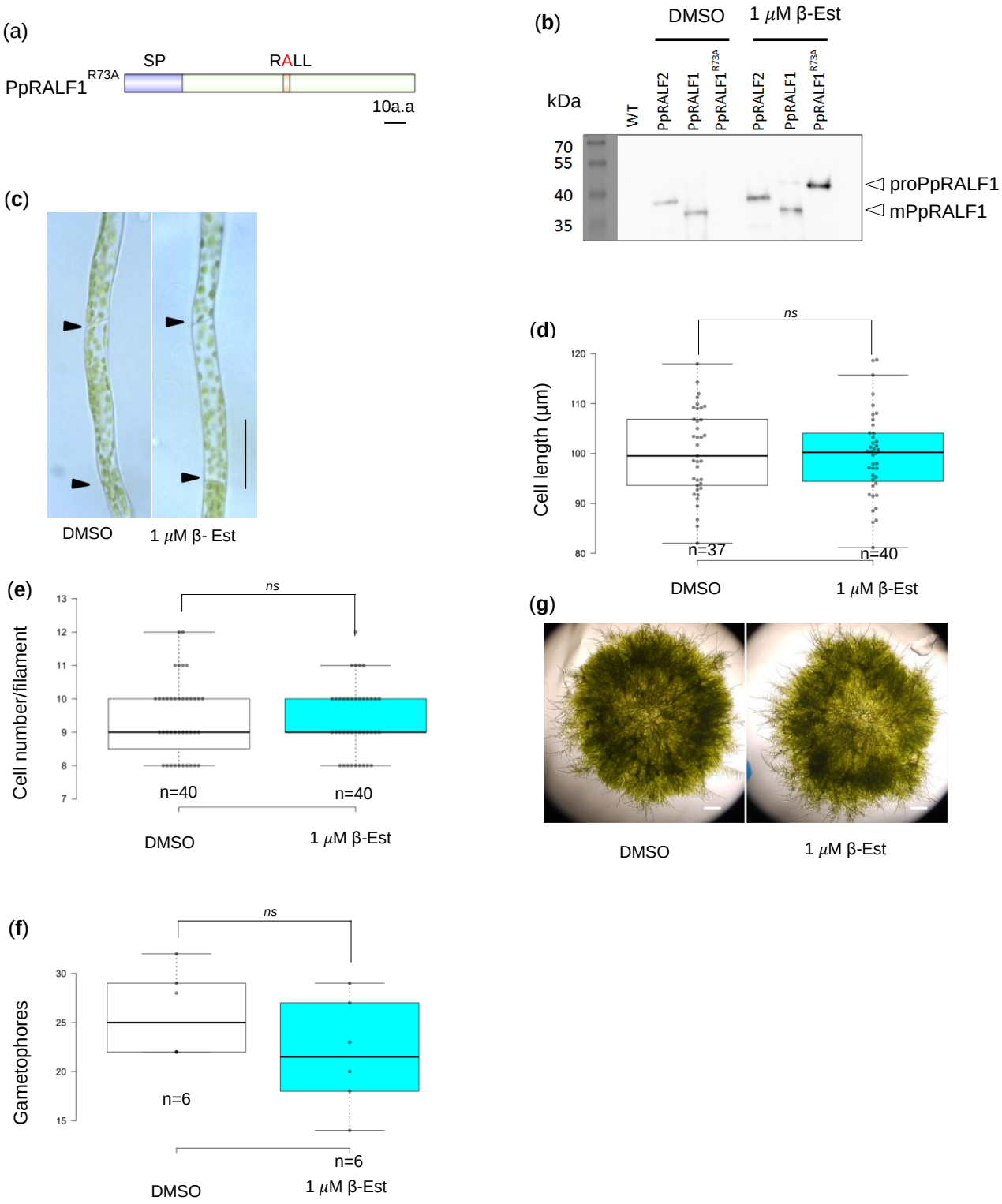

Figure 11. Active function of PpRALF1 requires proteolytic processing

(**a**) A schematic representation of PpRALF1^{R73A}. Red colored indicates the position of R73A mutation. Bar= 10 a.a.

(**b**) GFP immunoblot analysis of RALF1-Citrine, RALF1^{R73A}-Citrine, and RALF2-Citrine were induced by DMSO

or 1 μM β-estradiol. The molecular weight of ladder in kDa was shown on the numbers on the left. White arrow heads indicate propeptide PpRALF1 (proPpRALF1) and mature PpRALF1 (mPpRALF1). (**c**) Representative images of 7-day-old protonemata from iOX: PpRALF1^{R73A}-Citrine (line #6). Chloronemata were incubated on DMSO or 1 M β-estradiol-supplemented BCDAT medium under red light condition. Black arrow heads indicate septum. Bars= 50 μm. (**d-f**) The box plot shows the cell length (**d**), cell number (**e**), and gametophores number of iOX:PpRALF1^{R73A}-Citrine (line #6) (white box: DMSO and cyan: 1 μM β-Est) (**f**) . The black horizontal line indicates the median value and the box represents the second and third quartiles. The upper and lower quartiles are represented as whiskers. One-way ANOVA and Tukey's post hoc test were used to determine significant difference at $p < 0.01$ (indicated by ***) or not significant (*n. s.*). n=sample size. Colony of iOX: PpRALF1^{R73A}-Citrine (line #6) on BCDAT medium **(g)**.

9. Supporting figures

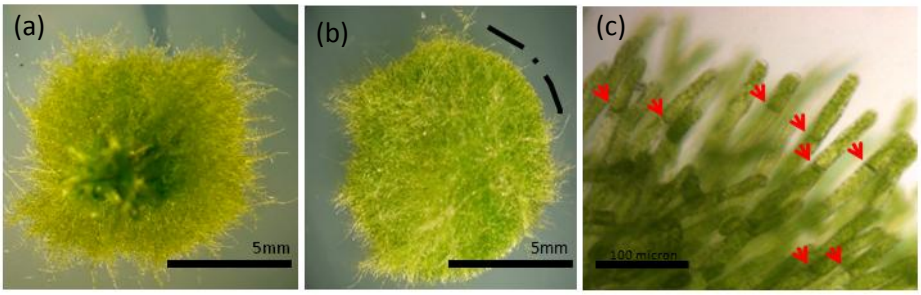

Supporting figure 1. Smooth edge feature is dominated by chloronemata cells in *Ppralf1KO*. Growth phenotype of colonies of WT (a) and *Ppralf1KO* (b and c) regenerated from a protoplast on BCDAT medium for 20 days. Dotted lines indicate smooth edge. Red arrows are septum of chloronemata cells. A scale bar is indicated on each panel.

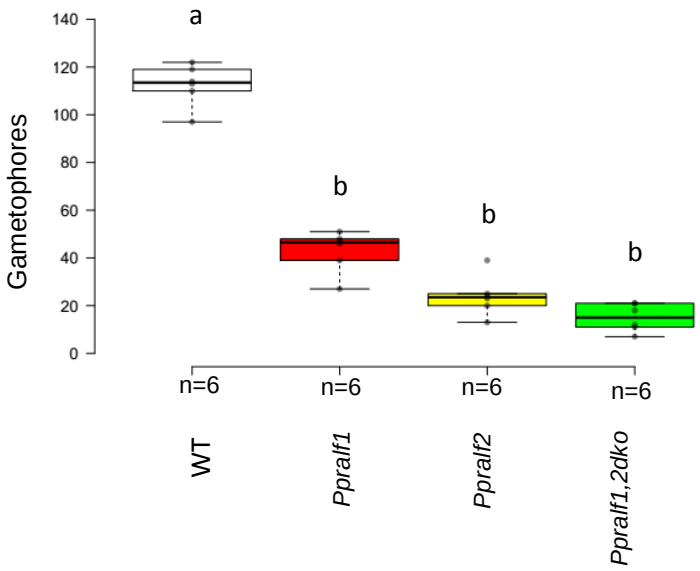

Supporting figure 2. Gametophore number of 30-day-old colonies of WT, *Ppralf1*, *Ppralf2*, *Ppralf1,2 dko*. The box plot shows the number of gametophore/colony in WT (white box), *Ppralf1* (red blox), *Ppralf2* (yellow box), *Ppralf3* (green box), *Ppralf1,2 dko* (blue box), *Ppralf2,3 dko* (orange box) and *Ppralf1,2,3 tko* (pink box). The black horizontal line indicates the median value and the box represents the second and third quartiles. The upper and lower quartiles are represented as whiskers. Letters indicate statistically significant differences (one-way ANOVA and Tukey's post hoc test, $p < 0.01$). n= sample size.

10. Supporting tables

Supporting table 1. Summary of oligonucleotides (primers) used in this study.

Number	Oligos (5'-3')	Purpose
#468	CGGGCCCCCCCTCGAGTGATCGGACTCGGTGCTCACTCAT	cloning of pTN182: PpRALF1-HR
#469	TATCGATACCGTCGACGTAACCCAGGCGTGACTCCCACCC	cloning of pTN182: PpRALF1-HR
#470	CATGCCCGGGTCTAGATGTTAAAGGGGGATTAACTCGG	cloning of pTN182: PpRALF1-HR
#471	GGCCGCTCTAGGATCCTGCATCATAAACAGCTCATTTGG	cloning of pTN182: PpRALF1-HR
#472	CATGCCCGGGTCTAGATGTTAAAGGGGGATTAACTCGG	cloning of p35S-Zeo: PpRALF2-HR
#473	GGCCGCTCTAGGATCCTGCATCATAAACAGCTCATTTGG	cloning of p35S-Zeo: PpRALF2-HR
#474	ATCCACTAGTTCTAGAATACAGTCCGAATTACTTCCTCAG	cloning of p35S-Zeo: PpRALF2-HR
#475	TATAGGGCGAATTGGAGCTCTGGTGGTGGATATTCTTGAAGGT	cloning of p35S-Zeo: PpRALF2-HR
#476	CGGGCCCCCCCTCGAGAGAAGACATACTTCATATCAATTA	cloning of pTN186: PpRALF3-HR
#477	TATCGATACCGTCGACTGTCAGGCAGTCAGGCAGTCGCA	cloning of pTN186: PpRALF3-HR
#478	CTAGACATATGGATCCAAGTGGTTACTAATGGCTACGTG	cloning of pTN186: PpRALF3-HR
#479	ACCGCGGTGGCGGCCGCACCCTCATGGCTCGTGCATGCGCA	cloning of pTN186: PpRALF3-HR
#499	AGTGTGACAATAGTAAAGCTTTTC	genotyping of *Ppralf3* knock-out
#500	AGTTGATGGAAGCCATCGTACTAC	genotyping of *Ppralf3* knock-out
#509	GTTCTCTCCGCTGGGAAACTCATC	genotyping of *Ppralf1* knock-out
#510	TCTTGTGAGACGAGAGAACGTGGA	genotyping of *Ppralf1* knock-out
#511	GTCACTCAATAGTTCTTGACAAAT	genotyping of *Ppralf2* knock-out
#512	TACAAATGCCATGAGTAATGCCAA	genotyping of *Ppralf2* knock-out

Supporting table 2. Transgenic lines are used in this study.

Transgenic lines	Antibiotics selection
Ppralf1	Geneticin
Ppralf2	Zeocin
Ppralf3	Hygromycin
Ppralf1, 2 dko	Geneticin, Zeocin
Ppralf2,3 dko	Zeocin, Hygromycin
Ppralf1,2,3 tko	Geneticin, Zeocin, Hygromycin
iOX: PpRALF1-Citrine	Hygromycin
iOX: PpRALF1R73A-Citrine	Hygromycin
iOX: PpRALF2-Citrine	Hygromycin
PpRALF1-Citrine (knock-in)	Geneticin
PpRALF2-tagRFP (knock-in)	Geneticin

11. Abbreviations

Abbreviations are used in this thesis:

CrRLK1L	: Catharantus roseus RLK1-like
d	: Day
DMSO	: Dimethyl sulfoxide
FER	: FERONIA
GFP	: Green fluorescent protein
HR	: Homologous regions
iOX	: Inducible overexpression
PRMB	: Protoplast regeneration medium for the bottom layer
PRMT	: Protoplast regeneration medium for the top layer
RALF	: Rapid alkalinization factor
RLK	: Receptor-like kinase
S1P	: Serine protease
β-Est	: β-Estradiol